Astron. Astrophys. 357, 520–526 (2000)

ASTRONOMY AND ASTROPHYSICS

BeppoSAX observations of the nearby low-mass X-ray binary and fast transient SAX J1819.3–2525

J.J.M. in 't Zand[1], E. Kuulkers[1,2], A. Bazzano[3], R. Cornelisse[1,2], M. Cocchi[3], J. Heise[1], J.M. Muller[1,4], L. Natalucci[3], M.J.S. Smith[1,5], and P. Ubertini[3]

[1] Space Research Organization Netherlands, Sorbonnelaan 2, 3584 CA Utrecht, the Netherlands
[2] Astronomical Institute, Utrecht University, P.O. Box 80000, 3508 TA Utrecht, the Netherlands
[3] Istituto di Astrofisica Spaziale (CNR), Area Ricerca Roma Tor Vergata, Via del Fosso del Cavaliere, 00133 Roma, Italy
[4] BeppoSAX Science Data Center, Nuova Telespazio, Via Corcolle 19, 00131 Roma, Italy
[5] BeppoSAX Science Operation Center, Nuova Telespazio, Via Corcolle 19, 00131 Roma, Italy

Received 17 November 1999 / Accepted 13 January 2000

Abstract. SAX J1819.3–2525 is a nearby X-ray transient which exhibited a fast and large X-ray outburst on Sep. 15, 1999 (Smith et al. 1999). The Wide Field Cameras and the Narrow Field Instruments (NFI) on board *BeppoSAX* observed SAX J1819.3–2525 at various stages of its activity before that, in the spring and fall of 1999. The fluxes range between 0.012 and 0.3 Crab units (2–10 keV). The NFI observation is unique because it is the longest semi-continuous observation of SAX J1819.3–2525 so far, and it offers a study of the spectrum at a relatively high resolution of 8% full width at half maximum at 6 keV. We discuss the observations with emphasis on the X-ray spectrum. A strong Fe-K emission line was detected in SAX J1819.3–2525 with an equivalent width between 0.3 and 1 keV. The line energy is up to 6.85±0.02 keV and suggests the presence of highly ionized iron. We identify this as fluorescent emission from a photo-ionized plasma. The continuum spectrum is typical for a low-mass X-ray binary in which emission from an accretion disk corona plays an important role. There is no sign of an eclipse or periodic signal due to the binary orbit in this exposure, despite the fact that the twin jets seen at radio wavelengths suggest a high inclination angle.

Key words: accretion, accretion disks – stars: binaries: close – stars: individual: SAX J1819.3–2525, XTE J1819–254, V4641 Sgr – X-rays: stars

1. Introduction

The X-ray source SAX J1819.3–2525 was discovered in February, 1999, independently with the Wide Field Cameras (WFCs) on *BeppoSAX* (In 't Zand et al. 1999a) and with the Proportional Counter Array (PCA) on *RossiXTE* (ergo, its alternative designation XTE J1819–254, Markwardt et al. 1999a). The WFC detection involved an hour-long flare with a peak of 80 mCrab on Feb. 20. The first PCA detection occurred during regular scans of the Galactic Center field, on Feb. 18.

Send offprint requests to: J.J.M. in 't Zand (jeanz@sron.nl)

For some time there was confusion over the identification of the optical counterpart. The variable star GM Sgr is within the 2′-radius WFC error box of the X-ray source as noted by In 't Zand et al. (1999a). However, it was later discovered that the actual counterpart is another, previously unknown, variable star only ∼1′ north of GM Sgr: V4641 Sgr (Williams 1999, Samus et al. 1999).

V4641 Sgr was found to show a large outburst in visual magnitude $m_{\rm V}$ from about 11 on Sep. 14.8 up to 8.8 on Sep. 15.4 (Stubbings 1999). X-ray observations with the All-Sky Monitor on *RossiXTE* also showed a bright outburst of SAX J1819.3–2525 up to a peak intensity of 12.2 Crab on Sep. 15.7 (2–12 keV, Smith et al. 1999). The giant X-ray outburst was preceded by a 4.5 Crab precursor 0.8 d earlier. Between both peaks the flux decreased to a quiescent level. Wijnands & Van der Klis (2000) report that during the tail of the giant X-ray outburst, strong variability was observed of factor-of-four on seconds time scales to factor-of-500 on minutes time scales. The giant outburst was also seen at radio wavelengths (Hjellming et al. 1999a, 1999b, 1999c). The radio source was resolved and had the appearance of a twin jets structure extending 0.25″ each jet. An HI absorption experiment against the radio source indicates an approximate distance of 0.5 kpc. We will adhere to this distance in the present paper although the uncertainty may be as large as 50%. The giant and precursor outburst were, furthermore, seen in 20–100 keV (McCollough et al. 1999).

Within 2 d after the giant outburst, V4641 Sgr settled down to a quiescent brightness of $m_{\rm V} = 13.5$. Combined with the failure of any X-ray detection since the giant outburst (C.B. Markwardt, priv. comm.), this shows that the flaring activity faded considerably, although the Balmer lines continued to show additional activity up to at least Sep. 30 (Garcia et al. 1999, Wagner 1999). With a 0.5 kpc distance, the giant outburst would have a peak X-ray luminosity of 8×10^{36} erg s^{-1} in 2–10 keV. This luminosity, and the spectrum discussed in the present paper, clearly suggest that there is a compact object at play that is either a neutron star or black hole. The optical counterpart identifies the object as a low-mass X-ray binary (LMXB), and the short distance implies

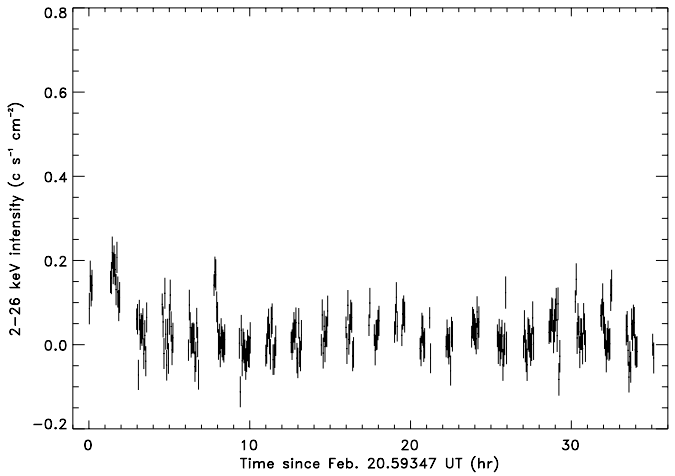

Fig. 1. Light curve of first flare on Feb. 20, as measured with the WFC unit 1 in the 2 to 26 keV band. The time resolution is 200 s.

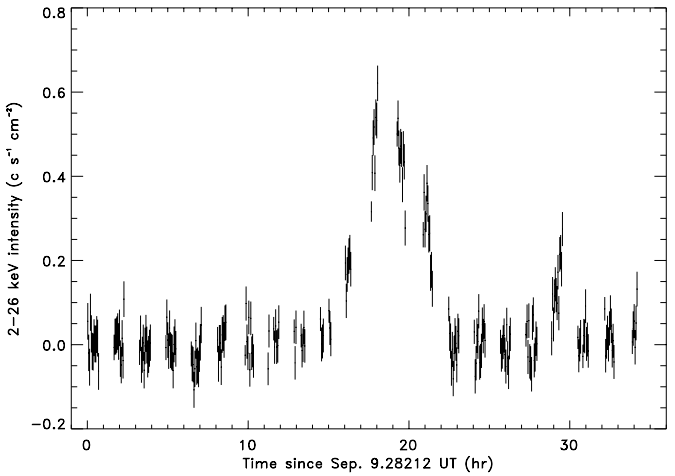

Fig. 2. Light curve of first flare on Sep. 10, as measured with the WFC unit 2 in the 2 to 26 keV band. The time resolution is 200 s.

it is possibly the *nearest* LMXB known so far (c.f., Van Paradijs & White 1995). This opens up interesting perspectives for SAX J1819.3–2525 as a case study of the quiescent emission from transient low-mass X-ray binaries. We note that recently Rutledge et al. (1999) introduced diagnostics for the nature of the compact object from the quiescent emission.

In this paper, we present the observations of SAX J1819.3–2525 with the WFCs and Narrow Field Instruments (NFI) on *BeppoSAX* in the spring and fall of 1999. This includes the longest semi-continuous observation of the system so far. SAX J1819.3–2525 was observed in two states: a flaring state with peak fluxes that are one to two orders of magnitude less than that of the giant outburst, and a 'calm' state with an average flux that is about three orders of magnitude smaller (though still considerably higher than that of the quiescent emission).

2. Observations

The *BeppoSAX* platform carries two sets of astrophysical X-ray and γ-ray devices in space (Boella et al. 1997a). One pertains to two identical Wide Field Cameras (WFCs, Jager et al. 1997) that view the sky with 40×40 square degrees field-of view in opposite directions with $5'$ spatial resolution in the 2 to 26 keV bandpass. The other set includes the Narrow Field Instruments (NFI) that are co-aligned in a direction that is perpendicular to that of both WFCs. The NFI include two imaging instruments that are active below 10 keV, the Low-Energy and the Medium-Energy Concentrator Spectrometer (LECS and MECS respectively, see Parmar et al. 1997 and Boella et al. 1997b respectively), and two non-imaging instruments that have bandpasses of ~ 12 to 300 keV (the Phoswich Detector System or PDS, Frontera et al. 1997) and 4 to 120 keV (the High-Pressure Gas Scintillation Proportional Counter or HP-GSPC, Manzo et al. 1997). The MECS has a photon energy resolution of 8% (full width at half maximum) at 6 keV.

Since mid 1996, the WFCs carry out a long-term program of monitoring observations in the field around the Galactic center. The program consists of campaigns during the spring and fall of each year. Each campaign lasts about two months and typically comprises weekly observations. SAX J1819.3–2525 was detected twice during these campaigns so far, in hourly exposures above a $\sim$50 mCrab detection limit, on Feb. 20 and Sep. 10, 1999. The first WFC-detection triggered a target-of-opportunity observation (TOO) with the NFI on March 13.22–14.02, 1999 (this is 186 d before the giant outburst). SAX J1819.3–2525 was strongly detected in three NFI (the HP-GSPC was not turned on), and the average intensity was found to be about 12 mCrab (2–10 keV). The NFI net exposure times on SAX J1819.3–2525 are 10.2 ks for LECS, 27.7 ks for MECS and 14.7 ks for PDS. The LECS and MECS images show a single bright source, the position as determined from the MECS image is R.A. $18^{\rm h}19^{\rm m}22\farcs2$, Decl. = $-25^\circ24'03''$ (Eq. 2000.0, error radius $0\farcm8$) which is $1\farcm0$ from that determined with the WFC (In 't Zand et al. 1999a) and $0\farcm4$ from the optical counterpart V4641 Sgr.

3. Light curves

The background-subtracted light curves of the two flares as measured with the WFCs are presented in Figs. 1 and 2. Besides these two occasions, the source was never detected in either short 1-hr or long 24-hr WFC exposures with typical upper limits of 50 and 12 mCrab respectively. The light curves of both detections are characterized by sporadic flaring activity up to 0.2 ct cm^{-2} s^{-1}, which corresponds to 0.1 Crab units, with a larger and longer flare on Sep. 10 with a peak of 0.3 Crab units. The large flare was above the detection limit for about 6 hr and occurred in the middle of a 34 hr long observation. It started on Sep. 10.0, which is 5.4 d before the giant outburst. Its duration is comparable to that of the giant flare.

The flaring activity on a time scale of hours is in line with the behavior as measured with the Proportional Counter Array (PCA) on *RossiXTE* (Markwardt et al. 1999b). The PCA covers SAX J1819.3–2525 bi-weekly since Feb. 5, 1999, for individual snapshot exposures of about 60 s with a sensitivity of about 1 mCrab. SAX J1819.3–2525 was first seen on Feb. 18 and

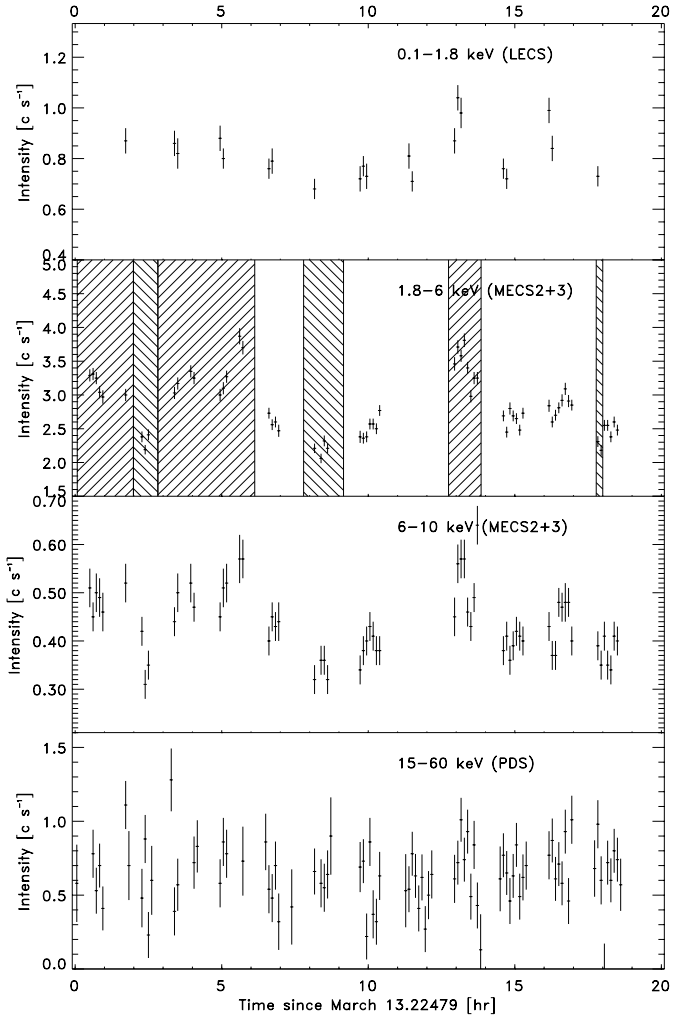

Fig. 3. Light curve as measured with the NFI in a number of bandpasses, corrected for background. The time resolution is 400 s. In the second panel from above the time intervals have been hatched that refer to low-flux intervals (\\ hatched) or high-flux intervals (// hatched).

subsequently showed an erratic variable behavior until immediately after the giant outburst, with fluxes ranging from 0.5 to 30 mCrab (Markwardt et al. 1999b). Since the giant outburst, no emission was detected anymore (C.B. Markwardt, priv. comm.).

The WFC data do not reveal any type I X-ray burst from SAX J1819.3–2525 in about 0.8 Ms of source coverage for the year 1999 when it was seen to be active with the PCA (Markwardt et al. 1999b), or for ∼3 Ms over all WFC observations since 1996.

Fig. 3 shows the evolution of the background-corrected photon count rates in various bandpasses of the three NFI, in 400 s time resolution. For an explanation of the method of data extraction, we refer to In 't Zand et al. (1999b). The light curves show slow variability on a time scale of a few hours with an amplitude of about 50%. The average flux level is 12 mCrab (2–10 keV) which, relative to the flares, can be regarded as calm emission. However, we note that this cannot be regarded as quiescent emission because the PCA has seen flux levels from this source at least one order of magnitude smaller (Markwardt et al. 1999b).

Table 1. Best-fit parameter values of the Comptonized model to the NFI spectrum. The last line specifies the $\chi^2_{\rm r}$ value for the fit without a bb (black body) component. This value applies after re-fitting the remaining parameters. EW means equivalent width.

Model	Comptonized + 2 narrow lines + black body
$N_{\rm H}$	$(0.05 \pm 0.02) \times 10^{22}$ cm^{-2}
bb kT	1.12 ± 0.09 keV
bb $R/d_{10\ {\rm kpc}}$	1.8 ± 0.3 km
Wien $kT_{\rm W}$	0.36 ± 0.02 keV
Plasma $kT_{\rm e}$	17 ± 6 keV
Plasma optical depth τ	1.5 ± 0.6 for disk geometry 3.6 ± 0.9 for spherical geometry
Comptonization parameter y	0.3 ± 0.1 for disk geometry 1.7 ± 0.4 for spherical geometry
Emission line energies	6.68 and 6.96 keV (fixed)
Emission line widths	0 keV (fixed)
Flux line 6.68 keV	$(2.8 \pm 0.9) \times 10^{-4}$ phot s^{-1} cm^{-2}
Flux line 6.96 keV	$(3.8 \pm 0.9) \times 10^{-4}$ phot s^{-1} cm^{-2}
EW line 6.68 keV	102 eV
EW line 6.96 keV	164 eV
Error in combined EW	30 eV
$\chi^2_{\rm r}$	1.30 (96 dof)
Flux (2–10 keV)	2.7×10^{-10} erg s^{-1} cm^{-2}
Flux (0.4–120 keV)	5.4×10^{-10} erg s^{-1} cm^{-2}
$\chi^2_{\rm r}$ without bb	2.06 (98 dof)

A power density spectrum of the MECS photon count rate, generated with a timing resolution of 0.02 s and averaged over 256 s time intervals, reveals no measurable narrow features nor broad-band noise. The upper limit on the variability, integrated between 0.01 and 10 Hz with power laws with indices of –0.5, –1.0 and –2.0, are 18, 8 and 3.5% fractional rms respectively (90% confidence). The upper limit on the pulsed amplitude is 1.3% fractional rms (95% confidence) in 0 to 25 Hz.

4. Spectrum of calm emission

We first extracted a spectrum for the average emission over the whole NFI observation. The spectral channels were rebinned so as to sample the spectral full-width at half-maximum resolution by three bins and to accumulate at least 20 photons per bin. The bandpasses were limited to 0.4–4.0 keV (LECS), 1.8–10.5 keV (MECS) and 15–120 keV (PDS) to avoid photon energies where either the spectral calibration of the instruments is not complete or no flux was measured above the statistical noise. We tried to model the spectrum with various descriptions. In all models, an allowance was made to leave free - within reasonable limits - the relative normalization of the spectra from LECS and PDS to that of the MECS spectrum, to accommodate cross-calibration uncertainties in this respect. Publicly available instrument response functions and software were used (version November 1998).

The continuum could best be fitted ($\chi^2_{\rm r} = 1.30$ for 96 dof) with a Comptonization model (Titarchuk 1994) plus black body radiation, see Table 1. Next to that there is a strong emission line at 7 keV. A fit with a single narrow line results in a centroid

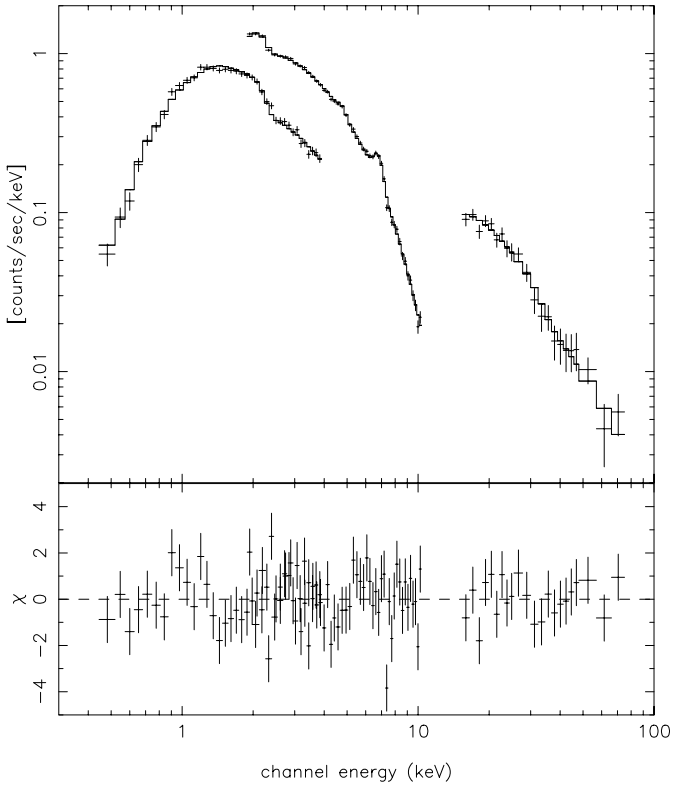

Fig. 4. Upper panel: count rate spectrum (crosses) and Comptonized spectrum model (histogram) for the average emission. Lower panel: residual in units of sigma per channel.

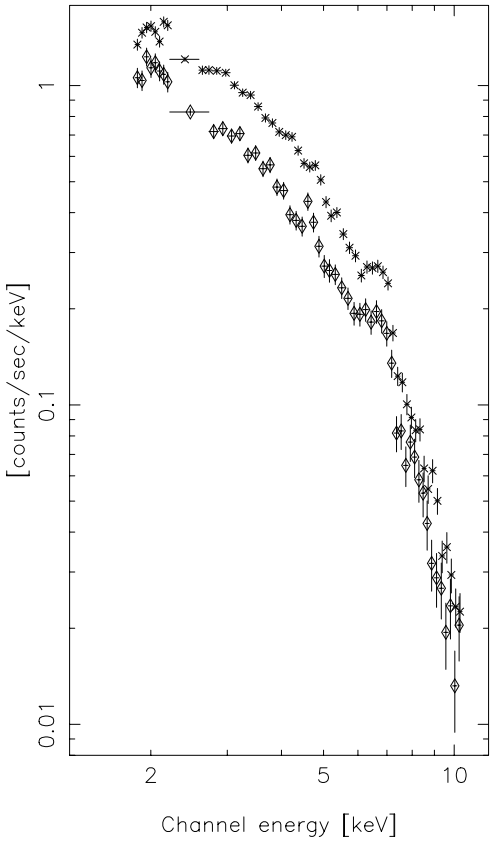

Fig. 5. Average MECS spectrum for the low-flux (lower) and high-flux intervals (upper) of the data (see also Fig. 3).

energy of 6.85 ± 0.02 keV. We identify this as Kα fluorescence in strongly ionized iron. The centroid energy is between the expected Fe-K lines for helium-like (6.68 keV) and hydrogen-like Fe (6.96 keV). We included in the model narrow lines at these fixed energies. The best-fit parameter values are given in Table 1 and a graph of the spectrum and the model fit in Fig. 4. The fits with other continuum models, in combination with a black body and two narrow line components results in fit qualities of $\chi^2_{\rm r} = 3.19$ for 98 dof (thermal bremsstrahlung), $\chi^2_{\rm r} = 1.83$ for 96 dof (broken power law) and $\chi^2_{\rm r} = 1.59$ for 96 dof (power law with high-energy cut off).

Terada et al. (1999) reported about the 1996 transient AX J1842.8–0423 which exhibited an Fe-K line at 6.80 keV with a large equivalent width of 4 keV. The 0.5–10 keV continuum plus line spectrum was successfully fitted with a thin hot thermal plasma emission model of temperature 5.1 keV. We fitted such a model according to the MEKAL code implementation (Mewe et al. 1995). The fit was reasonable, provided two additional components were included. With a power law and black body as additional components, $\chi^2_{\rm r} = 1.73$ (98 dof), which is a worse fit than the Comptonization model in Table 1. The resulting plasma temperature is 9.1 ± 0.5 keV. The fitted contribution of the thin plasma to the flux is of order 10%. The emission measure of the thermal plasma is $(2.08 \pm 0.13) \times 10^{56} (d/0.5\ {\rm kpc})^2$ cm^{-3}.

E(B–V)=+0.24 (Wagner 1999) implies $N_{\rm H} = 0.13 \times 10^{22}$ cm^{-2} according to the relationship defined by Predehl & Schmitt (1995). If we assume that the uncertainty in E(B–V) is 0.10, where most of the uncertainty comes from the uncertainty in the calibration of the relationship used by Wagner (1999) between the equivalent width of the 578.0 nm interstellar absorption line to E(B–V) (see Herbig 1975), then the error in $N_{\rm H}$ is 0.05×10^{22} cm^{-2}. If we fix $N_{\rm H}$ to 0.08×10^{22} cm^{-2} and leave free the remaining parameters of the Comptonized model in Table 1, $\chi^2_{\rm r}$ is 1.31 (97 dof). We conclude that $N_{\rm H}$ as determined from the X-ray spectrum is consistent with E(B–V)=+0.24$\pm$0.10.

To determine whether the variability as illustrated in Fig. 3 is accompanied by strong spectral changes, we extracted a spectrum for times when the source was relatively faint and one for times when the source was relatively bright. These times are indicated by hatched areas in Fig. 3. Subsequently, we employed the same Comptonized model as for the whole observation, leaving free only the normalizations of the different contributions. The resulting values for $\chi^2_{\rm r}$ are 1.36 for the bright data (104 dof) and 1.22 (103 dof) for the faint data. The 44% difference in the 0.4–10 keV flux between the faint and bright data is due to approximately equal changes in blackbody and Comptonized components (i.e., 25 and 19% respectively). The flux of the emission lines scales with the integral flux: the combined equivalent widths of both lines is identical in both cases at 0.26 keV. This spectral behavior is illustrated in Fig. 5 which zooms in on the MECS part of the spectrum (including the emission lines)

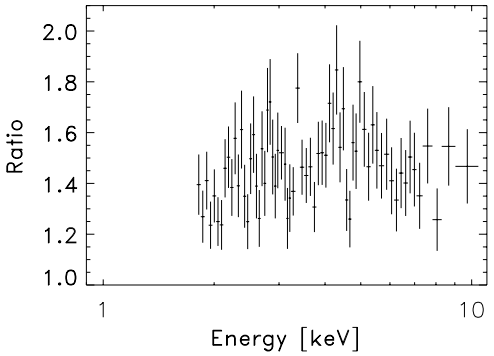

Fig. 6. Ratio of count rate spectrum between bright and faint selections of NFI data. The binning was arranged such that the error per data point is less than 10%.

for the two extremes. In Fig. 6 the ratio between both spectra is presented. This is consistent with a constant ratio of 1.44 ± 0.02 throughout the spectrum ($\chi^2_{\rm r} = 1.18$ for 65 dof). The apparent bump between 4 and 5 keV is statistically not significant.

5. Spectrum of flare

We extracted a 2–26 keV spectrum of the complete Sep. 10 flare which amounts to an elapsed time of 5.5 hr and an exposure time of 2.3 hr, and attempted to fit the same Comptonization model as applies to the NFI data when the source is ~ 20 times fainter. Leaving free only the normalizations of the different spectral components, the fit was unsatisfactory with $\chi^2_{\rm r} = 2.59$ for 24 dof. However, if $N_{\rm H}$ was allowed to vary, the fit became dramatically better with $\chi^2_{\rm r} = 0.89$ (23 dof) and $N_{\rm H} = (2.5 \pm 0.4) \times 10^{22}$ cm^{-2}. If instead the black body temperature was allowed to vary, an even better improvement occurred with $\chi^2_{\rm r} = 0.64$ (23 dof) and k$T_{\rm bb} = 2.4 \pm 0.2$ keV. If the Fe-K emission lines at 6.68 and 6.96 keV are replaced for a single one whose energy is left free, the fit improves further to $\chi^2_{\rm r} = 0.50$ for 23 dof. The line energy then is 6.39 ± 0.18 keV. This suggests a shift of the ionization balance to a lower degree (Fe I-XVII). We determined an average flux over the 3 hr duration of the peak of 5×10^{-9} erg cm^{-2} s^{-1}. The equivalent width of the emission line is 1.0 ± 0.3 keV. The flare spectrum is presented in Fig. 7.

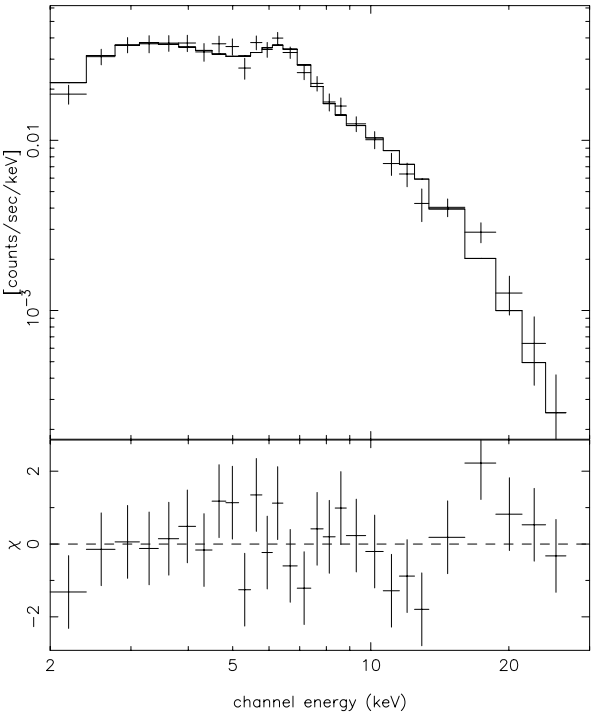

Fig. 7. Spectrum of the second flare and the fit with the Comptonized model with black body component of temperature k$T = 2.4$ keV and an emission line at 6.4 keV. The lower panel presents the residuals in units of sigma per channel.

6. Discussion

We have analyzed the spectrum at basically two flux levels which correspond to 2–10 keV luminosities of $8 \times 10^{33} (d/0.5\ {\rm kpc})^2$ erg s^{-1} and $2 \times 10^{35} (d/0.5\ {\rm kpc})^2$ erg s^{-1}, where d is the distance to SAX J1819.3–2525. These compare to a maximum luminosity during the giant outburst of $8 \times 10^{36} (d/0.5\ {\rm kpc})^2$ erg s^{-1} (Smith et al. 1999) and a minimum of $6 \times 10^{32} (d/0.5\ {\rm kpc})^2$ erg s^{-1} (see below). These numbers may be multiplied by a factor of 2 to obtain a rough extrapolation of the X-ray luminosity to the 0.4–120 keV range. They show that, though bright, SAX J1819.3–2525 in fact has a peak luminosity that is at least an order of magnitude below the Eddington limit for a mass of the compact object that is equal to or larger than that of a canonical 1.4 M$_\odot$ neutron star. However, one should bear in mind that the sampling of the ASM light curve is sparse (about ten 90 s observations per day) and we do not know what the source did between ASM measurements.

The eye-catching feature of the *BeppoSAX* data is the strong Fe-K emission line complex. The line energies during the calm phase point to a large ionization degree of the iron. Two origins for the line can be considered: thermal emission from a thin hot plasma, where iron atoms are collisionally excited, or fluorescent emission from a plasma illuminated by the continuum X-radiation. The thin hot plasma model gave an unsatisfactory fit to the NFI data. Also, the fact that no difference was seen in equivalent width between the low- and high-flux intervals of the NFI data seems to be at odds with a thin thermal plasma origin of the emission line. Therefore, we believe it is more probable that we are dealing with fluorescent emission in a photo-ionized medium. The ionization degree of the medium is fairly high, the ionization parameter $\xi = L/nr^2$ (Kallman & McCray 1982), where r is the size of the fluorescent material and n the atom density, is of order 10^3 to 10^4 which implies that the medium must be close to the source of the continuum radiation.

The 2 to 26 keV spectrum of the second WFC-detected flare (Fig. 7) shows an ionization balance of iron that is at much lower degrees than that of the calm emission half a year earlier. Apparently, ξ is at least two orders of magnitude smaller. This implies that n and/or r increased substantially. Therefore, the cloud of fluorescent material must have been, during the flare, denser and/or farther away from the source of the fluorescing radiation (probably near to the compact object). The same probably ap-

plies to the giant outburst 5 days later because the iron line was seen at an energy of 6.5 keV then (Markwardt et al. 1999b).

We do not detect K-edge absorption of iron at the appropriate energies of 8.8 (Fe XXV) and 9.3 keV (Fe XXVI). The 3σ upper limit on the relative depth of an edge at 9.0 keV is 0.2 which does not appear to be very constraining (c.f., Makishima 1986).

The equivalent width of the Fe-K line complex is relatively large. In the WFC-detected flare in September, it was 3 to 4 times as large as during the March NFI observation. Markwardt et al. (1999b) also observed the Fe-K complex during the tail of the giant flare, at a photon energy that is close to that measured with WFC six days earlier and with an equivalent width of about 500 eV. Model calculations of the structure of the accretion disk coronae and data analyses of Fe-K lines in other X-ray binaries by Vrtilek et al. (1993) suggest that large equivalent widths in Fe-K lines may be due to high (edge-on) inclination angles. This appears to be in line with the high inclination angle inferred from the radio jets.

Hjellming et al. (1999b) reported a double-sided jet structure from SAX J1819.3–2525 in a VLA image taken on Sep. 16.02 UT, with sizes of roughly $0.25''$ in both directions. A subsequent VLA image taken on Sep. 17.93 only shows one of the two jets at the same position. If v is the intrinsic velocity of the jets, i the angle between the jets and the line of sight, and c the velocity of light, then the angular proper motion $\mu_\pm$ of the approaching (–) and receding jet (+) are given by:

$$\mu_\pm \; = \; (v/d)\sin i/[1 \pm (v/c)\cos i]$$

(e.g., Hjellming & Rupen 1995). We can only make a rough estimate of μ_+ and μ_-. The uncertainty results from the facts that no moving radio blobs were seen, like in GRO J1655–40 (c.f., Hjellming & Rupen 1995), and that no difference was measured between μ_+ and μ_- (this is partly due to insufficient accuracy of the position of the optical counterpart). If we assume that the difference between μ_+ and μ_- is less than 10%, we find that $(v/c)\cos i < 0.048$. The value for $\mu_+ \approx \mu_-$ is determined by the time of jet ejection. Depending on whether one takes this to be at the time of the measured optical peak (Stubbings 1999), X-ray peak or X-ray pre-peak (see Smith et al. 1999), the travel time of the jets on Sep. 16.02 was between 0.3 and 1.1 d. This results in an allowed range for $\mu_+ \approx \mu_-$ of 224 to 806 mas d^{-1}. This implies $(v/c) > 0.53$. The above constraint on $(v/d)\cos i$ then results in $i > 84.8°$. Additionally, we can obtain a constraint on the distance from $(v/c) < 1$ and $v \sin i = \mu\, d$. For $\mu = 224$ mas d^{-1}, $d < 0.8$ kpc. Conversely, a distance of 0.5 kpc implies a jet ejection on Sep. 15.3 for $v = c$ or Sep. 14.7 for $v = 0.53c$.

The angle i is probably close to the inclination angle of the binary orbit, since one may expect the jets to be ejected close to perpendicular to the binary's orbital plane. The high value of i then suggests that at times the compact object should be eclipsed by the companion star. Our NFI data involve the longest continuous observation ever performed of SAX J1819.3–2525 while it was above the detection threshold (all *RossiXTE* TOOs lasted shorter than 3 hr). During 19 hr no eclipse was seen. Since the earth obscured the view to SAX J1819.3–2525 each *BeppoSAX* orbit, there is some uncertainty in the non-detection of an eclipse. With this reservation, the non-detection suggests that either the binary has an orbital period in excess of 19 hr, or the jets are misaligned from the orbital rotation axis by more than $\sim 10°$ (like seems to be the case for the micro quasar GRO J1655–40, see Van der Hooft et al. 1997).

The X-ray flux of SAX J1819.3–2525 behaved quite erratic. Whenever SAX J1819.3–2525 was detected, it exhibited at least 50% variability on hourly time scales. The variability is not (quasi) periodic. The scan observations with the PCA show that the source turned on probably on Feb. 18 and disappeared immediately after the giant outburst on Sep. 15. During the seven months in between, the snapshot measurements revealed fluxes varying at least between an upper limit of 0.4 and detections of up to 12×10^{-10} erg cm^{-2} s^{-1} (2–60 keV; Markwardt et al. 1999b, C.B. Markwardt priv. comm.). The two WFC-detected flares show that the flux sometimes reached flux levels one order of magnitude higher. Where does this variability come from and why did it turn off immediately after the giant outburst?

The mass transfer from the companion star should be mediated either through an (irregular) wind from the companion star or an accretion disk. Which one applies to SAX J1819.3–2525 is unclear, given the observations thus far. The high variability is perhaps most easily explained by an irregular wind from the companion star. Such wind accretion is very common among the high-mass X-ray binaries (see review by White et al. 1995). We note that SAX J1819.3–2525 shows similarities to CI Cam. CI Cam was fast (e-folding decay time 0.6 d, Harmon et al. 1998), exhibited a bright Fe-K line (EW up to 597 eV, Orr et al. 1998), was a radio jet source (Hjellming & Mioduszewski 1998), and was detectable in the 20–70 keV band (Harmon et al. 1998). The optical counterpart of CI Cam is a symbiotic B star with an irregular wind. The alternative, in the accretion disk interpretation, is that disk or thermal instabilities are continuously important. The apparent 0.3 to 0.9 day head start in the giant outburst of the optical to the X-ray emission suggests that a disk instability may be at work during this particular flare which moves from the outside to the inside of the disk, like has been seen in dwarf novae (e.g., Meyer & Meyer-Hofmeister 1994) and in the LMXB black-hole transient GRO J1655–40 (Orosz et al. 1997). During the 5 days before the giant outburst V4641 Sgr is continuously 2 mag brighter than immediately after the giant outburst when there is hardly any X-ray emission (Kato et al. 1999). This can be explained as optical emission from a disk which disappeared with the giant outburst. The alternative in the wind accretion interpretation is that the 2 mag come from the companion star. This too is not unreasonable, increased levels of mass loss are likely to go hand in hand with such brightening. Finally, there is the observation that the largest flare forced the system to go in quiescence. Again, this can be explained either way. In the accretion disk interpretation, the giant outburst drained the disk in such a manner that no accretion occurs anymore. The implied time scale of this drainage is about 10 hr. This can only be explained if the drained mass is small though large enough to induce a strong flare.

The short distance enables one to set a rather strict limit on the flux for the quiescent emission. The PCA monitoring program reveals that the flux went below an upper limit of 0.4×10^{-10} erg cm^{-2} s^{-1} (2–60 keV) or 1 mCrab (C.B. Markwardt, priv. comm.). Assuming the same spectrum holds as during our NFI observation (when the flux was approximately 25 times higher), the 0.4–120 keV luminosity upper limit is $< 12\times10^{32}(d/0.5\ \mathrm{kpc})^2$ erg s^{-1}. Unfortunately, this flux limit is too high to say something sensible about the nature of the compact object (see, e.g., Rutledge et al. 1999).

We reiterate the point made by Wijnands & Van der Klis (2000) that this transient may be an example of a separate class of fast and faint X-ray transients whose existence has been proposed by Heise et al. (1999) and is characterized by peak luminosities that are two orders of magnitude less than the typical bright soft X-ray transient and by outburst durations of order one week instead of months. Heise et al. estimate a rate of 18 such transients per year within 20° from the Galactic center. Such transients are easily over-seen by surveying instruments with small duty cycles if they are at the usual few-kpc distances. It is only because of its brightness due to its nearness that SAX J1819.3–2525 was easily noticed. At the distance to the Galactic center, the source would only have had a peak flux of 40 mCrab.

It is not clear whether the compact object is a neutron star or a black hole candidate. No X-ray characteristics that unambiguously identify the nature, such as type I X-ray bursts or pulsations, are present. Optical Doppler measurements during quiescence will give the best opportunity to obtain constraints on the mass of the compact object.

Acknowledgements. We thank Frits Paerels for useful discussions. This research has made use of linearized and cleaned event files from the ASI-BeppoSAX SDC on-line database and archive system. *BeppoSAX* is a joint Italian and Dutch program.

References

Boella G., Butler R.C., Perola G.C., et al., 1997a, A&AS 122, 299
Boella G., Chiappetti L., Conti G., et al. 1997b, A&AS 122, 327
Frontera F., Costa E., Dal Fiume D., et al. 1997, A&AS 122, 357
Garcia M.R., McClintock J.E., Callanan P.J., 1999, IAUC 7271
Harmon B.A., Fishman G.J., Paciesas W.S., 1998, IAUC 6874
Heise J., in 't Zand J.J.M., Smith M.J., et al. 1999, in proc 'The Extreme Universe' (3rd Integral Workshop), eds. A. Bazzano, G.G.C. Palumbo, C. Winkler, Astrophys. Lett. Comm. 38, 297
Herbig G.H. 1975, ApJ 196, 129
Hjellming R.M., Rupen M.P., 1995, Nat 375, 464
Hjellming R.M., Mioduszewski, A.J., 1998, IAUC 6872
Hjellming R.M., Rupen M.P., Mioduszewski A.J., 1999a, IAUC 7254
Hjellming R.M., Rupen M.P., Mioduszewski A.J., 1999b, IAUC 7265
Hjellming R.M., Rupen M.P., Mioduszewski A.J., et al. 1999c, AAS Meeting 195, 134.03
In 't Zand J.J.M., Heise J., Bazzano A., et al. 1999a, IAUC 7119
In 't Zand J.J.M., Verbunt F., Strohmayer T.E., et al. 1999b, A&A 345, 100
Jager R., Mels W.A., Brinkman A.C., et al., 1997, A&AS 125, 557
Kallman T., McCray R. 1982, ApJS 50, 263
Kato T., Uemera M., Stubbings R., Watanabe T., Monard B. 1999, IBVS 4777
Makishima K. 1986, in "The Physics of Accretion onto Compact Objects", eds. K.O. Mason, M.G. Watson, N.E. White (Berlin: Springer Verlag), p. 249
Manzo G., Giarusso S., Santangelo A., et al. 1997, A&AS 122, 341
Markwardt C.B., Swank J.H., Marshall F.E.., 1999a, IAUC 7120
Markwardt C.B., Swank J.H., Morgan E.H., 1999b, IAUC 7257
McCollough M.L., Finger M.H., Woods P.M., 1999, IAUC 7257
Mewe R., Kaastra J.S., Liedahl D.A. 1995, Legacy 6, 16
Meyer F., Meyer-Hofmeister E. 1994, A&A 288, 175
Orosz J.A., Remillard R.A., Bailyn C.D., McClintock J.E., 1997, ApJ 478, L83
Orr A., Parmar A.N., Orlandini M., et al. 1998, A&A 340, L19
Parmar A.N., Martins D.D.E., Bavdaz M., et al. 1997, A&AS 122, 309
Predehl P., Schmitt J.H.M.M. 1995, A&A 293, 889
Rutledge R.E., Bildsten L., Brown E.F., Pavlov G.G., Zavlin V.E. 1999, ApJ 514, 945
Samus N.N., Hazen M., Williams D., Welther B., Williams G.V., 1999, IAUC 7277
Smith D.A., Levine A.M., Morgan E.H., 1999, IAUC 7253
Stubbings R. 1999, IAUC 7253
Terada Y., Kaneda H., Makishima K., et al., 1999, PASJ 51, 39
Titarchuk L. 1994, ApJ 434, 313
Van der Hooft F., Groot P.J., Shahbaz T., et al. 1997, MNRAS 286, L43
Van Paradijs J., White N.E. 1995, ApJ 447, L34
Vrtilek S.D., Soker N., Raymond J.C., 1993, ApJ 404, 696
Wagner R.M. 1999, IAUC 7276
White N.E., Nagase F., Parmar A.N., 1995, in "X-ray Binaries", eds. W.H.G. Lewin, J. van Paradijs, E.P.J. van den Heuvel (Cambridge University Press, Cambridge), p. 1
Wijnands R., van der Klis M. 2000, ApJ 528, L93
Williams G.V. 1999, IAUC 7253